

36. Dubey, A. K., Koyama, Y., Hashimoto, N., Fujita, O. (2019). Effect of geometrical parameters on thermo-acoustic instability of downward propagating flames in tubes. *Proceedings of the Combustion Institute*, 37 (2), 1869–1877. doi: <https://doi.org/10.1016/j.proci.2018.06.155>
37. Volkov, V. E. (2014). Mathematical simulation of laminar-turbulent transition and the turbulence scale estimation. *Odes'kyi Politechnichnyi Universytet. Pratsi*, 2, 155–159. doi: <https://doi.org/10.15276/opu.2.44.2014.27>
38. Volkov, V. E. (2016). Two-dimensional flame instability and control of burning in the half-open firechamber. *Automation of Technological and Business Processes*, 8 (1), 21–27. doi: <https://doi.org/10.21691/atbp.v8i1.18>

An assessment of the feasibility of using the existing equipment of a rotary kiln cooler drum for heat treatment of a carbon-containing filler to produce synthesis gas using production waste in the form of a dust fraction of heat-treated petroleum coke or anthracite is carried out. A mathematical model of the process of gasification of carbon particles is formulated in the continuous-discrete formulation, including thirteen global reactions, of which four are heterogeneous and nine are homogeneous. A numerical model of gasification of a dust fraction of a carbon-containing filler in the rotary kiln cooler drum in the axisymmetric formulation is developed. The convergence of the numerical solution of the gasification problem by the grid step is investigated. It is found that the computational grid, which includes 73,620 cells and 75,202 nodes, leads to an error in determining the main parameters of the model of no more than 1–2%. Verification of the developed numerical model is performed. It is found that the difference between the molar fractions of CO and H₂, the values of which were obtained by various software products (Fluent, NASA CEA), is in the range of (2.8...5.8)%. Using the developed numerical model of the process of gasification of a carbon-containing filler in the rotary kiln cooler drum, the quantitative composition of the combustible components of the syngas for different initial parameters is determined. It is found that with the ratio O₂/C=(42.7...51.6)%, the predicted quantitative composition of the combustible gases of synthesis gas in molar fractions is CO=(32.8...36.9)%, H₂=(17.1...18.4)% and CH₄=(0.03...0.16)%. The possibility of using the NASA CEA program, intended for operational calculations of equilibrium chemistry, for engineering calculations of the material composition of synthesis gas of industrial furnace equipment, is shown

Keywords: rotary kiln, cooler drum, carbon-containing material, heat treatment, gasification, syngas, numerical simulation

UDC 662.741.3:66.041.49:004.942

DOI: 10.15587/1729-4061.2020.210767

DETERMINATION OF PARAMETERS OF THE CARBON-CONTAINING MATERIALS GASIFICATION PROCESS IN THE ROTARY KILN COOLER DRUM

A. Karvatskii

Doctor of Technical Sciences, Professor, Senior Researcher
Department of Chemical, Polymer and Silicate Engineering*

T. Lazariev

PhD, Leading Researcher
Yuzhnoye Design Office

Kryvorizhska str., 3, Dnipro, Ukraine, 49008

S. Leleka

PhD, Senior Researcher
Scientific Research Center

"Resource-saving Technologies"*

I. Mikulionok

Doctor of Technical Sciences, Professor, Senior Researcher
Department of Chemical, Polymer and Silicate Engineering*

O. Ivanenko

PhD, Associate Professor

Department of Ecology and Plant Polymers Technology*

E-mail: olenka.vasaynovich@gmail.com

*National Technical University of Ukraine

"Igor Sikorsky Kyiv Polytechnic Institute"

Peremohy ave., 37, Kyiv, Ukraine, 03056

Received date 18.06.2020

Accepted date 17.08.2020

Published date 31.08.2020

Copyright © 2020, A. Karvatskii, T. Lazariev, S. Leleka, I. Mikulionok, O. Ivanenko

This is an open access article under the CC BY license

(<http://creativecommons.org/licenses/by/4.0>)

1. Introduction

The significant cost of natural gas, as well as the need to comply with stringent environmental safety requirements of industrial enterprises, causes the transition of the energy sector and other industries to an increase in the use of solid fuel with its preliminary gasification. Gasification is known to be a process that involves the use of heat and water vapor to convert carbon-containing materials to syngas, which in-

cludes combustible gases such as carbon monoxide, hydrogen and methane.

This, in turn, led to the appearance of a large number of developments of reactor equipment for gasification and research of gasification of solid fuels and biomass, in particular, by numerical methods of computational hydrodynamics [1–13]. These works do not consider the use of existing industrial furnace equipment for solid fuel gasification processes. Thus, the use of synthetic gas obtained from the

gasification of carbon-containing materials in various industries using existing equipment is an urgent task and requires careful justification.

2. Literature review and problem statement

During the study of gasification processes, an important problem is chemical kinetics and mechanisms responsible for combustion processes and may include a large number of reaction components and elementary reactions [14]. To solve this problem of chemical kinetics, two main approaches are used, the first of which is based on detailed multi-stage chemical reactions [15, 16], and the second is based on the use of simplified global reactions with a significantly smaller number of both components and reactions.

The main disadvantages of the first approach are the need for significant computational resources and limited application: for laminar or supersonic combustion modes, that is, in conditions of rather slow chemistry and low interaction of kinetics with turbulent flows.

The main drawback of the second approach may be incorrect results of numerical simulation for more than two-stage reactions and the use of a combined model of finite velocity/vortex dissipation [14].

A good example of reducing the number of reactions can be the paper [17], which provides the reduced global mechanism of syngas burning, consisting of two stages instead of twenty multi-stage chemical reactions.

The papers [1–13] use an approach with a limited number of reactions, and above all, together with a combined model of finite velocity/vortex dissipation.

For the numerical analysis of gasification processes, two models are mainly used: continuous-discrete (Euler-Lagrange) and continuous-continuous (Euler-Granular Multiphase). In the continuous-discrete model, the Computer Fluid Dynamics (CFD) approach is used to describe the behavior of the gas mixture of reaction components, and for particulate matter, the Discrete Phase Models (DPM) or Discrete Element Methods (DEM). In the continuous-continuous model, the CFD approach is used to describe the behavior of both the gas and pseudo-solid phases. Moreover, for the solid phase, additional equations are written on the basis of the kinetic theory of the granular flow.

In almost all of these studies, turbulent gasification modes are described by Reynolds averaged Navier-Stokes equations (RANS) using standard or realizable $k-\varepsilon$ models).

In [1–6], DPM or Euler-Lagrange formulations are used to determine the main parameters of the gasification process of solid combustible material, while the papers [7, 9–13] are based on the Euler-Granular Multiphase or Euler-Euler formulations, and in [8] both models are used.

Numerical studies in the papers [3–5, 7–10, 12, 14, 17] were performed using ANSYS Fluent, CFX software products [18].

The Euler-Granular Multiphase formulation provides for solving a non-stationary problem with an integration step over a small scale time. Using the DPM model allows obtaining a solution to the problem in the stationary approximation in a relatively small number of iterations [18].

However, the use of the DPM formulation imposes severe restrictions on the volume fraction of the solid phase, which should not exceed 10% of the volume of the gas phase [18]. Moreover, to ensure stability in solving the problem, the ra-

tio of the mass flow rate of solid particles to the mass of gas should be ≤ 1 [3]. When using the Euler-Granular Multiphase formulation of the problem, these limitations are absent [18].

In [1], using the DPM model and the axisymmetric formulation of the problem, a numerical study of a gasifier with a captured stream of coal suspension is conducted. The coal gasification model is based on four heterogeneous and five homogeneous reactions. The effect of the O_2 /coal ratio on the distribution of velocity, temperature, and component concentration is studied. The results of numerical analysis are in satisfactory agreement with experimental data.

The paper [2] is also devoted to a numerical study of a gasifier with a type of feed of a coal suspension by a captured stream using the Euler-Lagrange model. The complex numerical model for simulating the coal gasification process is based on the division of a complex process into several simplified stages, such as suspension evaporation, coal devolatilization and two-phase reactions in combination with a turbulent flow and two-phase heat transfer. The model is based on seven reactions, of which four are heterogeneous, and the rest are homogeneous. The simulation results are compared with experimental data in the form of the O_2 /coal ratio. It is found that the calculated carbon conversion is consistent with the measured value. It is shown that in the case of an increase in the O_2 /coal ratio, the quality of the synthesis gas deteriorates, which is explained by the loss of heat through the gas generator and the uncertain kinetics of heterogeneous reactions.

A hydrodynamic numerical model of a two-stage gas-gas gasifier with a coal suspension, which is purged with oxygen and designed for use in modern power plants, is given in [3]. To simulate the flow of a coal suspension, the DPM model is used, with the help of which specific physical processes occurring with coal particles are monitored: the release of moisture and evaporation, the removal of volatile substances, oxidation and gasification. It is shown that the developed numerical model of gasification predicts the composition of syngas close to the values obtained by the model of a reactor with limited equilibrium. It is found that the conversion of coal particles is 100 % and 86 % for the first and second stages, respectively.

The coal gasification model proposed in [4] includes models of pyrolysis, coal gasification, and gas phase reactions using the Euler-Lagrange formulation. Numerical modeling using a coal gasification model is conducted on a gasifier with a captured flow of research scale. The effect of the air/coal ratio on gasification characteristics, such as the efficiency of carbon conversion per passage, the amount of semicoke, the calorific value of the gaseous product, and the efficiency of cold gas is studied. A comparison of calculated and experimental data shows that most of the characteristics of gasification performance are accurately identified using numerical simulation.

The paper [5] presents a comprehensive numerical 3D model of a two-stage gasifier for modeling the gasification of the coal suspension stream. To account for the turbulence of flows in the gasifier, a realizable $k-\varepsilon$ model is used. To account for the turbulent effect on the gas-phase reaction in the gasifier, the method of the assumed probability density function (probability density function (PDF)) is used. The movement of coal suspension particles is described in the Lagrange reference system taking into account processes such as water evaporation, removal of volatile and four heterogeneous reactions of coal particles. To combine the interaction

of the gas phase with solid particles, the “source of particles in the calculation cell” method is used. Calculations of the gasification process for an elevated pressure of 4.2 MPa show consistency with experimental data. It is found that with an increase in the concentration of coal suspension, the conversion of coal increases. As a result of increasing temperature, the CO concentration is growing rapidly, and the H₂ concentration is slightly reduced.

A three-dimensional model of the hydrodynamics of a double fluidized bed biomass gasification system using the Euler-Lagrange formulation is given in [6]. To simulate gas-solid particle flows in a double fluidized bed gasifier, the MP-PIC (multiphase particle-in-cell) method, which is an analogue of DPM, is used. The aim of this work is to find effective ways to improve the circulation of solids in the gasifier. Verification of the accuracy of the calculations using the developed numerical model of the gasifier is carried out by the double conversion method. Numerical studies at atmospheric pressure are carried out in order to determine the influence of the structural and technological parameters of the gasifier on the circulation rate of solid particles depending on their size, as well as the flow of water vapor and air.

The paper [7] is devoted to modeling coal gasification processes in a circulating fluidized bed gasifier using the Euler-Euler formulation. A standard $k-\epsilon$ model is used to simulate turbulent flow regimes of the gas phase, while solid phase simulations are based on the kinetic theory of granular flow. The global chemical model included eleven surface and volume type reactions. To select a rational kinetic reaction rate, a sensitivity analysis is performed on the gasification reaction of semicoke. The influence of the working temperature, the steam/coal and air/coal ratio on the composition of synthetic gas at the outlet of the gasifier is studied. It is shown that the obtained dependences of these parameters are consistent with published data, which confirms the applicability of the Euler-Granular Multiphase formulation for modeling the processes of coal gasification in a circulating fluidized bed gasifier.

The work [8] is devoted to a detailed study of the application of various Euler-Euler and Euler-Lagrange formulations (approaches) for modeling gasification processes. A detailed description and connection diagram of the gas flow with solid particles and chemical reactions of the two approaches are given separately. The chemical model includes thirty heterogeneous and homogeneous reactions. It is shown that the numerical models existing in the literature mainly include the Euler model with several liquids, the CFD-DEM (Discrete Element Methods) or MP-PIC (multiphase particle-in-cell) model. The paper also analyzes the corresponding advantages and limitations of these models.

In [9], the gasification process in a circulating fluidized bed gasifier with a combustion chamber power of 50 kW is studied. A 3D model of coal burning in air is developed based on the Euler-Euler formulation. The kinetic model includes fifteen global heterogeneous and homogeneous chemical reactions. Comparison of the results of numerical analysis with the experiment shows a satisfactory agreement of the data.

The paper [10] is devoted to 3D modeling of a full cycle of a circulating fluidized bed gasifier based on the Euler-Granular Multiphase formulation. The kinetic model includes sixteen global heterogeneous and homogeneous chemical reactions. Verification of the numerical model was carried out according to experimental data taken from other literary

sources. It is shown that the syngas from a circulating fluidized bed gasifier contains more CO and H₂ than the syngas from a bubbled fluidized bed gasifier.

It is shown in [11] that 2D modeling can't completely replace 3D modeling and can only be used for qualitative research. In this paper, a new pseudo-two-wiring approach to modeling is considered with the advantages of two-dimensional Cartesian and axisymmetric assumptions for modeling a gas-solid flow in a bubble fluidized bed based on the Euler-Euler formulation using free open-source MFIX software [19]. Comparison of the results of pseudo-two-world modeling and 2D analysis with experimental data shows the advantages of the first approach.

It is shown in [12] that an integrated combined gasification cycle with a trapped carbon stream is a viable technology for managing greenhouse gases using coal to generate electricity or produce hydrogen. Pilot equipment for coal gasification under pressure is described, as well as the possibility of modeling based on the Euler-Euler formulations to improve commercial technology for coal gasification. The chemical reaction model includes seven heterogeneous and homogeneous reactions. An approach to modeling gasification, its current forecast indicators and potential areas for further improvement are also presented. The results of numerical simulation are in good agreement with the data obtained using the NASA CEA program [20], intended for equilibrium chemistry calculations.

A mathematical model of physical and chemical processes that occur during solid fuel gasification in a fluidized bed reactor based on the Euler-Granular Multiphase formulations is given in [13]. The physical and chemical processes in the reaction zone of the gasifier are analyzed. The basic system of differential equations of continuum mechanics for a multiphase flow is formulated taking into account heat and mass transfer, turbulence and chemical reactions in the effective space of the gasifier. The physical equations of state of the medium and algebraic equations for calculating the coefficient of exchange between solid particles and the gas flow are given. The kinetic model includes ten global heterogeneous and homogeneous chemical reactions. The kinetic rates of chemical reactions of the gasification process are determined.

In the analyzed works [1–13], specialized equipment for the gasification of solid carbon-containing materials is considered and no attention is paid to the modernization of existing industrial equipment in order to produce synthetic gas. Moreover, the kinetics of the chemical reactions of gasification, presented in these papers, differ significantly. This applies both to the order of chemical reactions and activation energy, and especially to the values and dimensions of the pre-exponential factors of the Arrhenius kinetic equation, which makes their use very problematic.

Thus, the unresolved part of the considered problem is the expediency of using the synthetic gas obtained as a result of gasification of carbon-containing materials, in the conditions of operating production facilities of various industries. The analysis of this issue is considered based on the production of the carbon-containing filler of the electrode industry.

It is known that to obtain carbon-containing filler from petroleum coke or anthracite for the production of carbon products, rotary kilns are used, to maintain the temperature regime of which the heat from the combustion of natural gas is used. The technological regime of heat

treatment in these kilns is as follows [21]. From the cold end of the kiln drum, which has a certain inclination to the horizontal, raw material is supplied. Due to the inclination of the kiln drum and its rotation, the material gradually moves along the kiln and is subjected to heat treatment at temperatures above 1,200–1,300 °C due to the heat from the combustion of natural gas, as well as volatile and partially carbon-containing material. The material is unloaded from the hot end of the kiln, from the side of which the gas burners are installed along the axis of the kiln. The flue gases in the kiln drum move in the opposite direction to the movement of the material. After unloading, the heat-treated filler with a temperature of about 950 °C enters the rotary cooler drum of the kiln, where it is cooled and then goes to the storage hopper.

To reduce the consumption of natural gas in the production technology of carbon-containing filler, it is proposed to use syngas, for the generation of which it is necessary to use the modernized operating equipment of the kiln cooler drum, the dust fraction of the heat-treated material is captured by the smoke exhaust cyclones, as well as the heat of the material and flue gases.

At the same time, the modernization of the cooler drum consists in organizing a carbon dust fraction supply system together with water vapor and air diluted with hot flue gases entering the gasification process of the material particles. In addition, due to the rotation of the material in the cooler drum, a fine fraction of the heat-treated material is formed, which is also involved in the gasification process.

3. The aim and objectives of the study

The aim of the work is to analyze the feasibility of using the existing equipment of rotary kilns for heat treatment of carbon-containing materials to produce syngas using waste products in the form of a dust fraction of heat-treated petroleum coke or anthracite.

To achieve this aim, the following objectives are set:

- to formulate a mathematical model of the gasification process of carbon-containing material particles in the continuous-discrete formulation using global reactions of this process;

- to develop a numerical model of the gasification process of bulk carbon-containing material in the rotary kiln cooler drum in the axisymmetric formulation;

- to substantiate the feasibility of the gasification process of carbon-containing filler in the rotary kiln cooler drum and perform verification of the developed numerical model.

4. Mathematical model of the problem of gasification of carbon-containing material

The mathematical formulation of the problem of gasification of carbon-containing material based on DPM for a mixture of reacting gases, taking into account the turbulent flow regime, thermal radiation and interaction with a discrete solid phase, includes the RANS equation system, which contains equations of conservation of mass, conservation of momentum, transfer of chemical reaction components, energy conservation and two k - ε equations of the turbulence model for turbulent kinetic energy and its dissipation:

$$\left\{ \begin{aligned} \frac{\partial \bar{\rho}}{\partial t} + \nabla \cdot (\bar{\rho} \tilde{v}) &= S_{pm}; \\ \frac{\partial \bar{\rho} \tilde{v}}{\partial t} + (\bar{\rho} \tilde{v} \cdot \nabla) \tilde{v} &= -\nabla \bar{p} + \nabla \cdot \bar{\tau}_{eff} + \bar{\rho} g + S_{pv}; \\ \frac{\partial \bar{\rho} \tilde{Y}_k}{\partial t} + \nabla \cdot (\bar{\rho} \tilde{v} \tilde{Y}_k) &= \nabla \cdot \bar{J}_k + \bar{\omega}_k, \quad k = \overline{1, N}; \\ \frac{\partial \bar{\rho} \tilde{h}}{\partial t} + \nabla \cdot (\bar{\rho} \tilde{v} \tilde{h}) &= \bar{\omega}_T + \nabla \cdot \bar{p} + \nabla \cdot \left(\lambda \nabla T + \frac{\mu_t}{Sc_t} \nabla h \right) + \\ &+ \bar{\tau}_{eff} : \nabla v - \nabla \cdot \left(\rho \sum_{k=1}^N J_k h_k \right) + S_{rad} + S_{ph}; \\ \frac{\partial (\bar{\rho} k)}{\partial t} + \nabla \cdot (\bar{\rho} \tilde{v} k) &= \nabla \cdot \left[\left(\mu + \frac{\mu_t}{\sigma_k} \right) \nabla k \right] + \bar{\tau}_{eff} : \nabla \tilde{v} - \bar{\rho} \varepsilon; \\ \frac{\partial (\bar{\rho} \varepsilon)}{\partial t} + \nabla \cdot (\bar{\rho} \tilde{v} \varepsilon) &= \nabla \cdot \left[\left(\mu + \frac{\mu_t}{\sigma_\varepsilon} \right) \nabla \varepsilon \right] + \\ &+ C_{\varepsilon 1} \frac{\varepsilon}{k} (\bar{\tau}_{eff} : \nabla \tilde{v}) - C_{\varepsilon 2} \bar{\rho} \frac{\varepsilon^2}{k}; \\ \bar{p} &= \bar{\rho} \frac{R}{W} \tilde{T}, \end{aligned} \right. \quad (1)$$

where $\bar{\cdot}$, $\tilde{\cdot}$ – means that the value is averaged by Reynolds and Favre, respectively; $\bar{\rho}$ – density, kg/m³; t – time, s; ∇ – Hamilton operator, m⁻¹; \tilde{v} – velocity vector, m/s; \bar{p} – pressure, Pa;

$$\bar{\tau}_{eff} = (\mu + \mu_t) \left[\nabla \tilde{v} + \tilde{v} \nabla - \frac{2}{3} (\nabla \cdot \tilde{v}) I \right] - \frac{2}{3} \bar{\rho} k I$$

– effective stress tensor, Pa; μ – dynamic viscosity, Pa·s;

$$\mu_t = \bar{\rho} C_\mu \frac{k^2}{\varepsilon}$$

– turbulent viscosity, Pa·s; k – turbulent kinetic energy, J/kg; ε – dissipation rate of turbulent kinetic energy, J/(kg·s); I – unit tensor of the second rank; g – acceleration vector of gravity, m/s²; \tilde{Y}_k – mass fraction of the k -th component of the chemical reaction; N – number of reaction components;

$$\bar{J}_k = - \left(\bar{\rho} D_{m,k} + \frac{\mu_t}{Sc_t} \right) \nabla \tilde{Y}_k + D_{T,k} \frac{\nabla T}{T}$$

– vector of the diffusion turbulent flow of the k -th component, kg/(m·s); $D_{m,k}$ – mass diffusion coefficient of the k -th component of the mixture, m²/s;

$$Sc_t = \frac{\mu_t}{\rho D_t}$$

– Schmidt number; D_t – turbulent diffusion coefficient, m²/s; $D_{T,k}$ – coefficient of thermal diffusion of the k -th component of the mixture, kg/s; $\bar{\omega}_k$ – source due to the average reaction rate of the k -th component

$$\left(\sum_{k=1}^N \bar{\omega}_k = 0 \right), \text{ kg}/(\text{m}^3\text{s});$$

$$\tilde{h}_k = \int_{T_{ref,k}}^{\tilde{T}} c_{p,k} dT$$

– explicit enthalpy of the k -th component, J/kg; T – absolute temperature, K; $T_{ref,k}$ – absolute reference temperature, K; c_p – mass isobaric heat capacity, J/(kg·K);

$$\bar{\omega}_T = -\sum_{k=1}^N h_k^0(T_{ref,k})\dot{\omega}_k$$

– volumetric heat source due to combustion, W/m³; λ – thermal conductivity coefficient, W/(m·K); (\cdot) – operator of the double scalar product; S_{pm} , S_{pv} , S_{ph} – initial terms associated with the mass (kg/(m³·s)), bulk force (N/m³) and enthalpy (W/m³) of solid particles, respectively; S_{rad} – initial term associated with thermal radiation, W/m³; $C_{\varepsilon 1}=1.44$; $C_{\varepsilon 2}=1.92$; $C_{\mu}=0.09$; $\sigma_k=1.0$; $\sigma_\varepsilon=1.3$ – coefficients of the k - ε turbulence model.

The discrete phase equation system is recorded in the Lagrange reference system (2) and includes two equations: conservation of momentum and energy. The trajectories of motion of solid particles are determined by integrating the equation of balance of forces acting on the particle over pseudo-clockwise steps. The equation of conservation of energy of solid particles describes convective and radiation heat transfer between particles and a liquid medium, heat transfer during chemical reactions, removal of volatiles and evaporation of moisture [5, 18].

$$\begin{cases} \frac{d\mathbf{u}_p}{dt} = F_D(\mathbf{u} - \mathbf{u}_p) + \frac{g(\rho_p - \rho)}{\rho_p} + F; \\ m_p c_p \frac{dT_p}{dt} = hA_p(T_\infty - T_p) + f_h \frac{dm_p}{dt} h_{reac} + \varepsilon_p A_p \sigma (\theta_R^4 - T_p^4), \end{cases} \quad (2)$$

where \mathbf{u} – velocity vector of the gaseous medium, m/s; \mathbf{u}_p – velocity vector of solid particles m/s; $F_D(\mathbf{u} - \mathbf{u}_p)$ – resistance force related to the particle mass, m/s²;

$$F_D = \frac{18\mu C_D Re}{\rho_p d_p^2 24}, 1/s;$$

μ – dynamic viscosity of the gaseous medium, Pa·s; C_D – dimensionless coefficient of hydraulic resistance; ρ_p – density of solid particles; kg/m³; ρ – density of the gaseous medium; kg/m³; d_p – average diameter of solid particles, m;

$$Re = \frac{\rho d_p |\mathbf{u}_p - \mathbf{u}|}{\mu}$$

– Reynolds number; F – mass force related to the mass of the particle, m/s²; m_p – solid particle mass, kg; h – convective heat transfer coefficient, W/(m²·K); A_p – particle surface area, m²; T_∞ – local absolute temperature of the gas medium, K; T_p – absolute temperature of a solid particle, K; f_h – fraction of the heat of the surface reaction, absorbed by the solid part; h_{reac} – heat of the surface reaction, J/kg; σ – Stefan-Boltzmann constant, W/(m²·K⁴); ε_p – blackness degree of the particle; θ_R – radiation temperature, K.

The relationship between the continuum phase (gas mixture) and the discrete phase (solid part) is determined by tracking the exchange of mass, momentum and energy [3]. The corresponding terms are in the equations of system (1).

The total rate of surface reactions on solid particles according to the model of multiple surface reactions consists

of the volumetric velocity of the diffuse and kinetic rate of a chemical reaction. For first-order chemical reactions, the total rate of the i -th reaction is determined by the formula [5]

$$\frac{1}{R_i} = \frac{1}{R_{i,d}} + \frac{1}{R_{i,k}} \rightarrow R_i = \frac{R_{i,d} R_{i,k}}{R_{i,d} + R_{i,k}}, \quad (3)$$

where

$$R_{i,d} = C_i \frac{[(T_p + T_\infty)/2]^{0.75}}{d_p} p_i$$

– diffusion rate of the i -th reaction, kg/(m²·s); C_i – diffusion coefficient of the i -th reaction, kg/(m²·s·K^{0.75}·Pa); p_i – partial pressure of the gas reagent of the i -th reaction, Pa; $R_{i,k}$ – apparent kinetic rate of the i -th reaction (Arrhenius equation taking into account pressure), kg/(m²·s); A_k – pre-exponential factor (steric factor) of the i -th reaction, kg/(m²·s·K ^{β} ·Pa ^{m}); E_a – activation energy, J/kmol; R – universal gas constant, J/(kmol·K).

The apparent kinetic rate of the i -th reaction is determined by the formula

$$R_{i,k} = A_i T_p^\beta \exp\left(-\frac{E_a}{RT_p}\right) \left(\frac{p_i}{10^5}\right)^m, \quad (4)$$

where β , m – exponents.

The flow rate of the j -th component of the i -th reaction on the surface of a solid particle is determined by the formula [18]

$$\bar{R}_i = A_p \eta Y_j R_i, \quad (5)$$

where Y_j – mass fraction of surface components j in the particle; η – efficiency coefficient.

In the system of equations (2), in addition to the combustion and gasification processes, one can take into account the evaporation of moisture and the removal of volatiles from solid particles [18].

To describe the interaction between the kinetics of chemical reactions and turbulence of flows, a model of finite velocity or vortex dissipation according to the dependence is used [3, 18]

$$R = \min[R_{ch}, R_{mix}(k, \varepsilon, X_R, X_p)], \quad (6)$$

where R_{ch} – rate of a chemical reaction according to the Arrhenius law; R_{mix} – speed of turbulent mixing; k – turbulent kinetic energy; ε – rate of turbulent energy dissipation; X_R – mole concentration of the reaction reagent; X_p – mole concentration of the reaction product.

Four heterogeneous and nine homogeneous reactions are used to describe the gasification of particles of heat-treated petroleum coke [18]. Global heterogeneous (surface) reactions include the combustion of semicoke, as well as the gasification of CO₂, H₂O, and H₂ [5, 18] (Table 1). Global homogeneous (volumetric) reactions of the gasification process are given in Table 2.

As can be seen from Tables 1, 2, the coefficients of heterogeneous and homogeneous gasification reactions differ in both value and sometimes dimensionality, which complicates their use in practical calculations.

Table 1

Kinetic coefficients of heterogeneous reactions

No.	Reaction	Reaction order	A	$E_a, J/kmol$	m	Source
1	$C_{<S>}+0.5O_2 \rightarrow CO$	$[C_{<S>}]^0 [O_2]^1 (1)$	$300 \text{ kg}/(\text{m}^2 \cdot \text{s} \cdot \text{Pa}^{0.65})$	$1.3 \cdot 10^8$	0.65	[5, 18]
			$4.54 \cdot 10^{-7} \text{ Pa}^{-1} \cdot \text{s}^{-1}$	$1.105 \cdot 10^8$	0	[10]
			$8.71 \text{ m}/(\text{s} \cdot \text{K})$	$1.49 \cdot 10^8$	–	[2]
2	$C_{<S>}+CO_2 \rightarrow 2CO$	$[C_{<S>}]^0 [CO_2]^1 (1)$	$2224 \text{ kg}/(\text{m}^2 \cdot \text{s} \cdot \text{Pa}^{0.6})$	$2.2 \cdot 10^8$	0.6	[5, 18]
			$3.92 \text{ Pa}^{-1} \cdot \text{s}^{-1}$	$2.239 \cdot 10^8$	0	[10]
			$4.4 \text{ m}/(\text{s} \cdot \text{K})$	$1.62 \cdot 10^8$	–	[2]
3	$C_{<S>}+H_2O \rightarrow CO+H_2$	$[C_{<S>}]^0 [H_2O]^1 (1)$	$42.5 \text{ kg}/(\text{m}^2 \cdot \text{s} \cdot \text{Pa}^{0.4})$	$1.42 \cdot 10^8$	0.4	[5, 18]
			$5.95 \cdot 10^{-5} \text{ Pa}^{-1} \cdot \text{s}^{-1}$	$1.135 \cdot 10^8$	0	[10]
			$1.33 \text{ m}/(\text{s} \cdot \text{K})$	$1.47 \cdot 10^8$	–	[2]
4	$C_{<S>}+2H_2 \rightarrow CH_4$	$[C_{<S>}]^0 [H_2]^1 (1)$	$1.62 \text{ kg}/(\text{m}^2 \cdot \text{s} \cdot \text{Pa}^1)$	$1.5 \cdot 10^8$	1	[5, 18]
			$8.25 \cdot 10^{-9} \text{ Pa}^{-1} \cdot \text{s}^{-1}$	$6.716 \cdot 10^7$	0	[10]
			$0.12 \text{ m}/(\text{s} \cdot \text{K})$	$1.49 \cdot 10^8$	–	[2]

Table 2

Kinetic coefficients of homogeneous reactions

No.	Reaction	Reaction order	A	$E_a, J/kmol$	β	Source
1	$Vol+1.706O_2 \rightarrow CO_2+N_2++1.543H_2O$	(1.5)	$2.119 \cdot 10^{11} (\text{m}^3/\text{kmol})^{0.5} \text{s}^{-1}$	$2.027 \cdot 10^8$	0	[18]
2	$CO+0.5O_2 \rightarrow CO_2$	$[CO]^1 [O_2]^{0.25} [H_2O]^{0.5} (1.75)$	$2.239 \cdot 10^{12} (\text{m}^3/\text{kmol})^{0.75} \text{s}^{-1}$	$1.7 \cdot 10^8$	0	[18]
		$[CO]^1 [O_2]^{0.25} [H_2O]^{0.5} (1.75)$	$2.239 \cdot 10^{12} ((\text{m}^3/\text{kmol})^{0.75} \text{s}^{-1})$	$1.674 \cdot 10^8$	0	[22]
		$[CO]^1 [O_2]^{0.25} [H_2O]^{0.5} (1.75)$	$2.239 \cdot 10^{12} (\text{m}^3/\text{kmol})^{0.75} \text{s}^{-1}$	$1.674 \cdot 10^8$	0	[7]
		$[CO]^1 [O_2]^{0.5} [H_2O]^{0.5} (2)$	$1.3 \cdot 10^{11} (\text{m}^3/\text{kmol}) \text{s}^{-1}$	$1.255 \cdot 10^8$	0	[9]
		$[CO]^1 [O_2]^{0.25} (1.25)$	$1.237 \cdot 10^{10} (\text{m}^3/\text{kmol})^{0.25} \text{s}^{-1}$	$1.67 \cdot 10^8$	0	[10]
		$[CO]^1 [O_2]^{0.25} [H_2O]^{0.5} (1.75)$	$3.98 \cdot 10^8 (\text{m}^3/\text{kmol})^{0.75} \text{s}^{-1}$	$4.18 \cdot 10^7$	0	[23]
3	$CO+H_2O \rightarrow CO_2+H_2$	$[CO]^{0.5} [H_2O]^1 (1.5)$	$2.35 \cdot 10^{10} (\text{m}^3/\text{kmol})^{0.5} \text{s}^{-1}$	$2.88 \cdot 10^8$	0	[18]
		$[CO]^1 [H_2O]^1 (2)$	$2.78 \cdot 10^3 (\text{m}^3/\text{kmol}) \text{s}^{-1}$	$1.257 \cdot 10^7$	0	[10]
4	$CO_2+H_2 \rightarrow CO+H_2O$	$[CO_2]^1 [H_2]^{0.5} (1.5)$	$1.785 \cdot 10^{12} (\text{m}^3/\text{kmol})^{0.5} \text{s}^{-1}$	$3.26 \cdot 10^8$	0	[18]
		$[CO_2]^1 [H_2]^1 (2)$	$1.049 \cdot 10^8 (\text{m}^3/\text{kmol}) \text{s}^{-1}$	$4.545 \cdot 10^7$	0	[10]
5	$H_2+0.5O_2 \rightarrow H_2O$	$[H_2]^1 [O_2]^1 (2)$	$9.87 \cdot 10^8 (\text{m}^3/\text{kmol}) \text{s}^{-1}$	$3.1 \cdot 10^7$	0	[18]
		$[H_2]^1 [O_2]^1 (2)$	$1.08 \cdot 10^{13} (\text{m}^3/\text{kmol}) \text{s}^{-1}$	$1.264 \cdot 10^8$	0	[9]
		$[H_2]^1 [O_2]^1 (2)$	$1.08 \cdot 10^{13} (\text{m}^3/\text{kmol}) \text{s}^{-1}$	$1.255 \cdot 10^8$	0	[7]
		$[H_2]^1 [O_2]^{0.5} (1.5)$	$1.631 \cdot 10^{12} (\text{m}^3/\text{kmol})^{0.5} \text{s}^{-1}$	$2.852 \cdot 10^7$	-1.5	[10]
		$[H_2]^{0.25} [O_2]^{1.5} (1.75)$	$5.0 \cdot 10^{20} (\text{m}^3/\text{kmol})^{0.75} \text{s}^{-1}$	$1.25 \cdot 10^8$	-1	[23]
6	$H_2O \rightarrow H_2+0.5O_2$	$[H_2O]^1 (1)$	$2.06 \cdot 10^{11} \text{ s}^{-1}$	$2.78 \cdot 10^8$	0	[18]
		$[H_2]^{-0.75} [O_2]^1 [H_2O]^1 (1.25)$	$2.93 \cdot 10^{20} (\text{m}^3/\text{kmol})^{0.25} \text{s}^{-1}$	$4.09 \cdot 10^8$	-0.88	[23]
7	$CH_4+1.5O_2 \rightarrow CO+2H_2O$	$[CH_4]^{0.7} [O_2]^{0.8} (1.5)$	$5.012 \cdot 10^{11} (\text{m}^3/\text{kmol})^{0.5} \text{s}^{-1}$	$2.0 \cdot 10^8$	0	[18]
		$[CH_4]^{0.7} [O_2]^{0.8} (1.5)$	$5.01 \cdot 10^{11} (\text{m}^3/\text{kmol})^{0.5} \text{s}^{-1}$	$2.012 \cdot 10^8$	0	[9]
		$[CH_4]^{0.7} [O_2]^{0.8} (1.5)$	$1.613 \cdot 10^{13} (\text{m}^3/\text{kmol})^{0.5} \text{s}^{-1}$	$2.0 \cdot 10^8$	0	[10]
		$[CH_4]^{0.7} [O_2]^{0.8} (1.5)$	$1.59 \cdot 10^{13} (\text{m}^3/\text{kmol})^{0.5} \text{s}^{-1}$	$1.998 \cdot 10^8$	0	[23]
8	$CH_4+H_2O \rightarrow CO+3H_2$	$[CH_4]^{0.5} [H_2O]^1 (1.5)$	$5.922 \cdot 10^8 (\text{m}^3/\text{kmol})^{0.5} \text{s}^{-1}$	$2.09 \cdot 10^8$	0	[18]
		$[CH_4]^1 [H_2O]^1 (2)$	$3.1 \cdot 10^8 (\text{m}^3/\text{kmol}) \text{s}^{-1}$	$1.247 \cdot 10^8$	0	[10]
		$[CH_4]^1 [H_2O]^1 (2)$	$3.1 \cdot 10^{11} (\text{m}^3/\text{kmol}) \text{s}^{-1}$	$1.25 \cdot 10^8$	0	[23]
9	$CO+3H_2 \rightarrow CH_4+H_2O$	$[CO]^1 [H_2]^2 (3)$	$1.16798 \cdot 10^{16} (\text{m}^3/\text{kmol})^2 \text{s}^{-1}$	$3.9824 \cdot 10^8$	0	[10]

5. Numerical model of the gasification process of bulk carbon-containing material

For the numerical implementation of the mathematical model of the gasification process in the cooler drum, the ANSYS

Fluent software was used [18]. At the same time, a realizable $k-\epsilon$ model was used to model turbulent flows, and a discrete ordinates method (DOM) was used for thermal radiation. Kinetic coefficients of heterogeneous reactions are accepted according to [5, 18], and homogeneous ones according to [10, 18].

In order to minimize the requirements for computing resources, a numerical model of the process of gasification of the dust fraction of carbon-containing filler in the rotary kiln cooler drum is based on the axisymmetric formulation, the kind of boundary conditions (BC) of which is shown in Fig. 1.

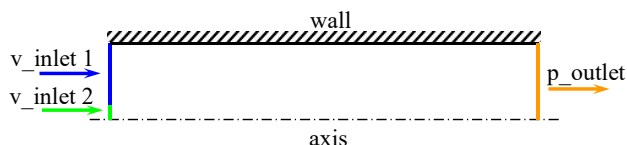


Fig. 1. Scheme of the types of BC of the numerical model of gasification of carbon-containing filler in the cooler drum in the axisymmetric formulation:

axis – drum symmetry axis; wall – solid wall; $v_{inlet 1}$, $v_{inlet 2}$ (velocity inlet) – inlet of flows at a given velocity; p_{outlet} (pressure outlet) – flow outlet; drum dimensions: diameter 1,400 mm, length 23,000 mm

According to the scheme (Fig. 1), the parameters of the numerical model of gasification were considered as follows:

- on $v_{inlet 1}$, the air flow strongly diluted with hot exhaust gases of a rotary kiln and water vapor with the chemical composition ($O_2=0.07$; $CO_2=0.05$; $H_2O=0.15$; $CO=0.08$ (wt.)) with a discrete change in axial velocity c (0.25, 0.5; 0.75; 1.0; 1.25; 1.5) m/s, temperature $T_1=853$ K and blackness degree of the boundary $\varepsilon_1=1$ was set;

- on $v_{inlet 2}$, the air flow with the addition of water vapor with the chemical composition ($O_2=0.15$; $CO_2=0.0$; $H_2O=0.25$; $CO=0.0$ (wt.)) with an axial velocity $v_2=2.5$ m/s, temperature $T_2=473$ K and blackness degree of the boundary $\varepsilon_2=1$ was set;

- on $v_{inlet 2}$, the flow of the discrete phase (dust fraction of carbon-containing filler with an equivalent diameter (100–300) μm), with an axial and radial velocity $v_{ax,D}=2.5$ m/s and $v_{r,D}=1.5$ m/s, respectively, at a temperature $T_D=300$ K was also set;

- on p_{outlet} , a pressure $p_{outlet}=0$ Pa and a temperature $T_{outlet}=800$ K of a return air flow with the chemical composition ($O_2=0.23$ (wt.)), the blackness degree of the boundary $\varepsilon_{outlet}=1$ were set;

- on wall, adhesion conditions for the gas flow, the blackness degree of the boundary $\varepsilon_{wall}=0.8$ and the BC for the energy equation of two types were set;

- the first type – BC of the I kind are set (Fig. 2), including a variable isothermal zone with a temperature $T_{wall}=1253$ K and a cooling zone with a linear law of temperature change from 1,253 K to 473 K;

- the second type – convective type BC (III kind) are set, taking into account a 50 mm thick fireclay refractory layer, which also simulate a hot zone (close to isothermal) with a length of 11.5 m.

In the case of setting the BC of the I kind, T_{wall} is determined by the temperature of the heat-treated bulk carbon-containing material that enters the cooler drum from the rotary kiln.

For the BC of the III kind, a hot zone with an ambient temperature $T_{env}=1,453$ K, heat transfer coefficient $\alpha_{env}=1,000$ W/($\text{m}^2\cdot\text{K}$) and a zone of water irrigation cooling with $T_{env}=300$ K and $\alpha_{env}=1,000$ W/($\text{m}^2\cdot\text{K}$) is set.

The gas medium in the numerical model was considered “gray”, and its absorption and scattering coefficients were

taken equal to each other and amounted to 5 m^{-1} , the refractive index was taken equal to 1.

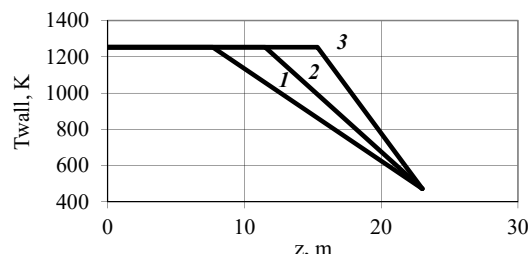


Fig. 2. Change in the temperature distribution along the length of the inner surface of the cooler drum (wall boundary in Fig. 1): 1 – length of the isothermal zone 7.67 m; 2 – 11.5 m; 3 – 15.33 m

The physical properties of the dust fraction of the carbon-containing filler were set as follows: true density 1,780 kg/m^3 ; mass isobaric heat capacity 1,000 J/($\text{kg}\cdot\text{K}$); the proportion of the combustible component 90 % (wt.); the fraction of volatiles 2 % (wt.); moisture content 4 % (wt.).

The thermophysical properties of fireclay refractory were adopted as follows: density 1,600 kg/m^3 ; thermal conductivity coefficient 1.5 W/($\text{m}\cdot\text{K}$); mass isobaric heat capacity 800 J/($\text{kg}\cdot\text{K}$).

The solution method is Pressure-Velocity Coupling with the first order of approximation of the convective terms of the equations of system (1).

Variation calculations according to the described numerical model were performed using a pseudo-non-stationary solver (Pseudo Transient) and automatic selection of the integration step over time. To obtain a stable solution for the temperature boundary conditions (BC of the I kind) on the inner surface of the cooler drum, it was necessary to perform 3,780 time steps, and for convection type BC (BC of the III kind) – about 7,560.

The convergence of the numerical solution of the gasification problem was carried out by the double conversion method. As a result, it was found that the computational grid, which includes 73,620 cells and 75,202 nodes, leads to an error in determining the main parameters of the model no more than 1–2 %.

To visualize the results of calculations of physical fields using the ANSYS Fluent software product, the free open software code ParaView was used [24].

6. Substantiation of the expediency of the process of gasification of carbon-containing filler in the rotary kiln cooler drum. Verification of the numerical model

Based on the developed numerical model of the gasification process for the dust fraction of carbon-containing filler in the rotary kiln cooler drum, a series of calculations was carried out to study the effect of the following parameters:

- changes in the oxidizer/carbon ratio (O_2/C);
- the length of the isothermal zone, type of boundary conditions;
- the presence of a refractory layer, and the like.

The results of these calculations determined the total mass fractions of O_2 , CO_2 , CO and H_2O at the inlet to the rotary kiln cooler drum, which, together with temperature and pressure, are needed to perform comparative

calculations of the gasification process using NASA CEA software [20] in the equilibrium chemistry approximation. Moreover, the O_2/C ratio was also calculated from the total mass flow rate of the oxidizing agent and the dust fraction of the carbon-containing filler at the inlet to the cooler drum.

The main combustible syngas gases are carbon monoxide, hydrogen and a small fraction of methane. That is why the comparison of calculations performed using the Fluent and CEA programs was performed for the indicated syngas components, including CO_2 .

Comparison results of calculations of the gasification process for the dust fraction of carbon-containing filler in the cooler drum at its outlet under boundary conditions of the I kind and the length of the isothermal zone of 11.5 m for different values of the O_2/C ratio are shown in Fig. 3.

As can be seen from Fig. 3–5, the results of calculations of the quantitative composition of the syngas at the cooler drum outlet for the length of the isothermal zone of 11.5 m according to various programs generally coincide. The smallest difference between the mole fraction of CO and H_2 is observed for the ratio $O_2/C=(42.7–51.6)$ % and is in the range of (3.6–5.8) %. Similar convergence is also observed for the length of the isothermal zone of the cooler drum of 7.67 m and 15.3 m.

A comparison of the dependences of the mole fractions of the syngas components at the outlet of the rotary kiln cooler

drum on the O_2/C ratio under boundary conditions of the I kind is shown in Fig. 6. These dependences are obtained using the Fluent and CEA software products.

According to the results of calculations using equilibrium chemistry ratios (Fig. 6, *b*), the maximum mole fractions of CO and H_2 in the syngas, provided that $CO_2 \approx 0$ %, is observed for the ratio $O_2/C=42.7$ %, while according to Fluent calculations under identical conditions, the extremum occurs only for the H_2 mole fraction (Fig. 6, *a*). With an increase in O_2/C , the mole fraction of the combustible constituents in the syngas decreases.

The results of calculations of physical fields during gasification of the dust fraction of carbon-containing filler under boundary conditions of the I kind performed using Fluent, are shown in Fig. 7, 8.

From Fig. 7, 8, it is clearly seen that the maximum mole fractions of the combustible components of the syngas are observed mainly in the cooling zone and in the outlet part of the drum, while non-combustible ones, on the contrary, are minimal. According to the calculations, the syngas cooler drum capacity at the O_2/C ratio=42.7 % under normal conditions is 1,509 m^3/h .

The dependence of the mole fractions of the main combustible components of the syngas on the length of the isothermal zone of the cooler drum obtained using the Fluent and CEA software products is shown in Fig. 9.

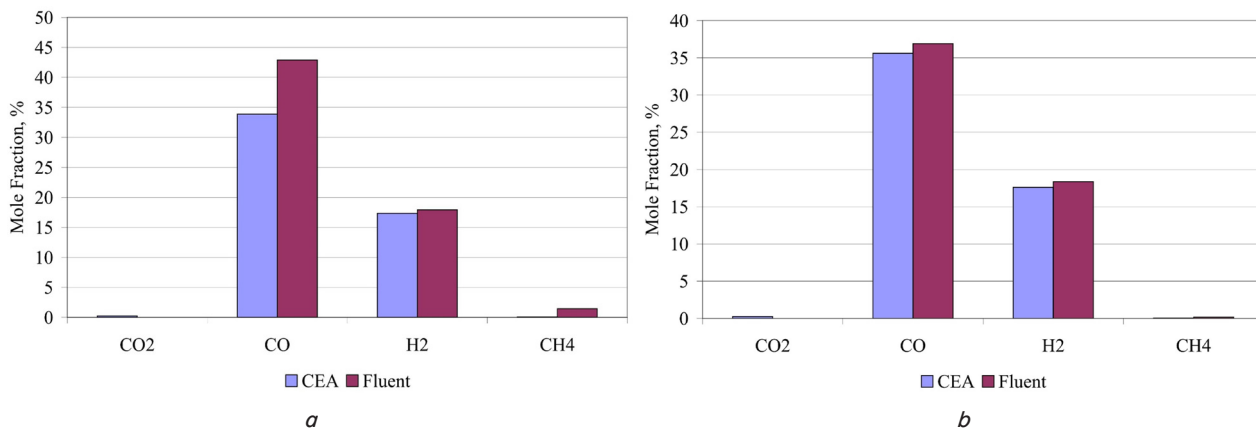


Fig. 3. Comparison of the quantitative composition of the syngas at the outlet of the rotary kiln cooler drum under boundary conditions of the I kind and length of the isothermal zone of 11.5 m for different values of the O_2/C ratio obtained using the Fluent and CEA software products: *a* – $O_2/C=37.2$ % (wt./wt.); *b* – $O_2/C=42.7$ %

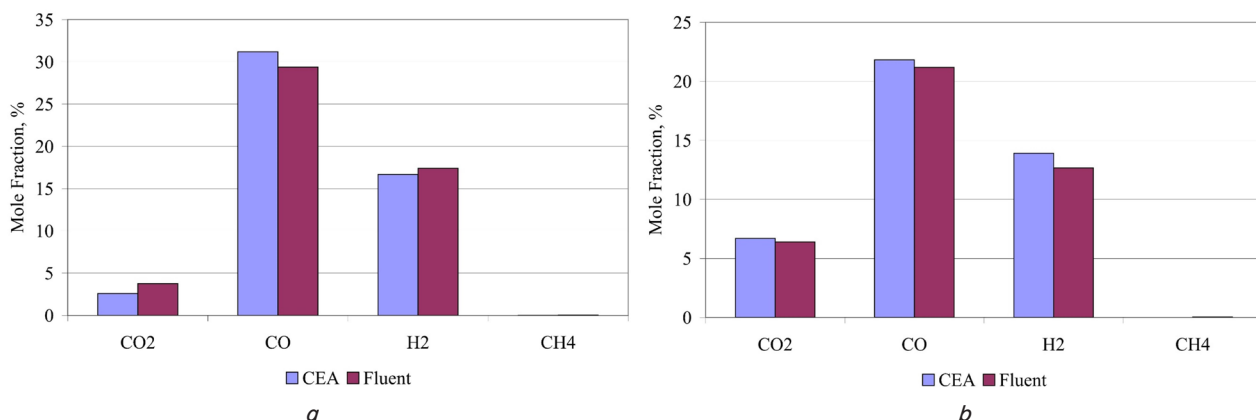


Fig. 4. Comparison of the quantitative composition of the syngas at the outlet of the rotary kiln cooler drum under boundary conditions of the I kind and the length of the isothermal zone of 11.5 m for different values of the O_2/C ratio obtained using the Fluent and CEA software products: *a* – $O_2/C=51.6$ %; (wt./ wt.); *b* – $O_2/C=70.7$ %

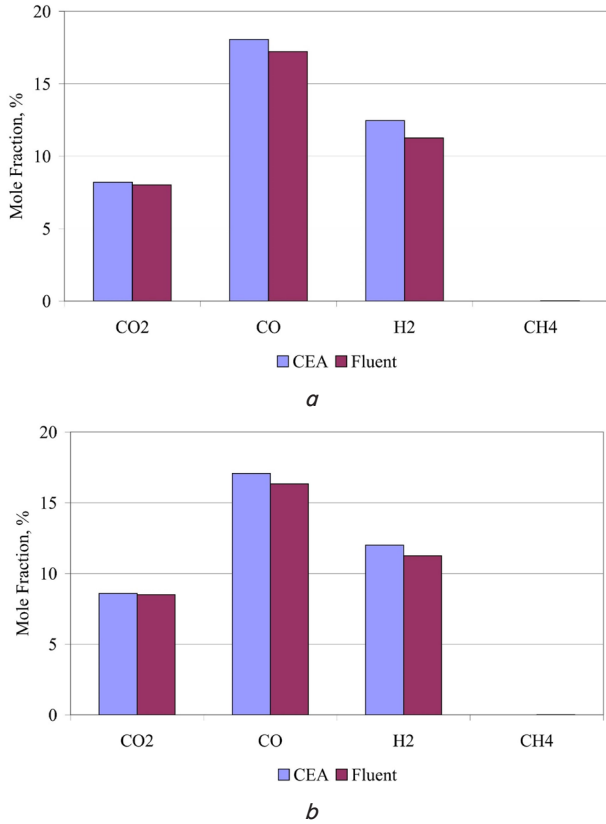


Fig. 5. Comparison of the quantitative composition of the syngas at the outlet of the rotary kiln cooler drum under boundary conditions of the I kind and the length of the isothermal zone of 11.5 m for different values of the O_2/C ratio obtained using the Fluent and CEA software products: *a* – $O_2/C=82.7\%$ (wt./wt.); *b* – $O_2/C=86.5\%$

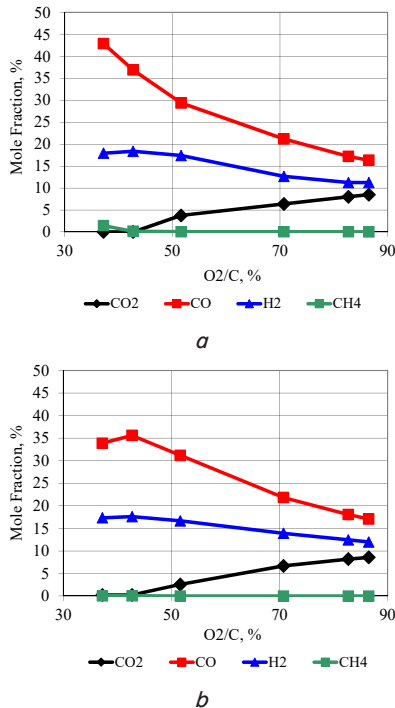


Fig. 6. Dependence of the mole fractions of the syngas components at the outlet of the rotary kiln cooler drum on the O_2/C ratio under boundary conditions of the I kind and length of the isothermal zone of 11.5 m: *a* – Fluent; *b* – CEA

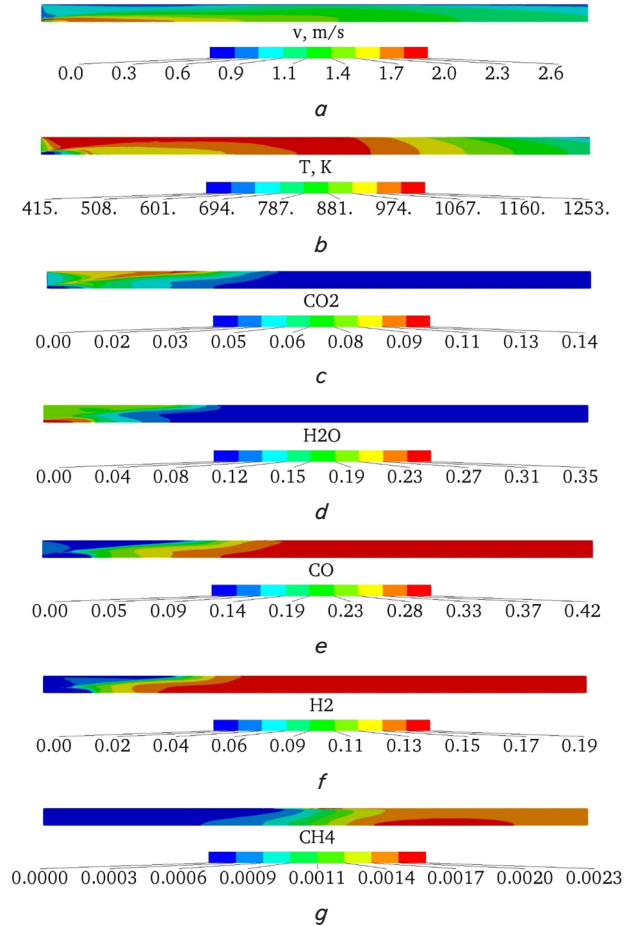


Fig. 7. Physical fields during the gasification of the dust fraction of carbon-containing filler under boundary conditions of the I kind and length of the isothermal zone of the drum of 11.5 m and the O_2/C ratio=42.7 %: *a* – velocity; *b* – temperature; *c* – CO_2 mole fraction; *d* – H_2O mole fraction; *e* – CO mole fraction; *f* – H_2 mole fraction; *g* – CH_4 mole fraction

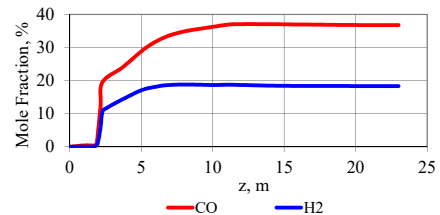


Fig. 8. Distribution of the molar fractions of the main combustible components of the syngas CO and H_2 along the axis of the cooler drum, boundary conditions of the I kind, the length of the isothermal zone of the drum of 11.5 m and the O_2/C ratio=42.7 %

The graphs in Fig. 9 show that the obtained results using various programs are in good agreement with each other and the value of the mole fractions of the main combustible components of the syngas is almost independent of the length of the isothermal zone of the cooler drum.

The calculation results of the gasification of the dust fraction of the carbon-containing filler in the cooler drum for convective-type BC taking into account the fireclay refractory layer on the drum are shown in Fig. 10–13.

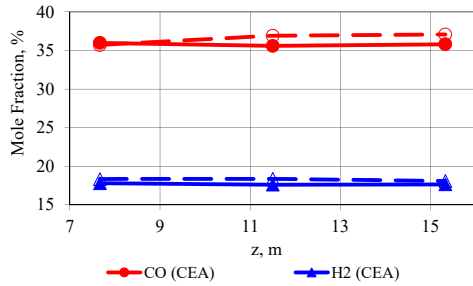


Fig. 9. Dependence of the mole fractions of CO and H₂ of the syngas on the length of the isothermal zone of the cooler drum for the O₂/C ratio=(42.4–44.2) % (wt./wt.) at the maximum yield of H₂ and minimum concentrations of CO₂=0 % and H₂O≈0 % according to Fluent and CEA calculations

The results of variant calculations for convective-type BC show that with an increase in the length of the hot zone of the cooler drum, the temperature of the syngas at its outlet increases significantly, which causes an increase in the temperature of the bulk material, and a decrease leads to a significant drop in the temperature of the gasification process and, accordingly, the yield of combustible components of the syngas.

The decisive influence on the gasification process in the cooler drum is played by the temperature of the heat-treated bulk material coming from the rotary kiln. To increase the efficiency of using the heat of the material coming from the rotary kiln, the thickness of the refractory in the hot (reaction) zone of the cooler drum should be greater than in the zone of its irrigation cooling.

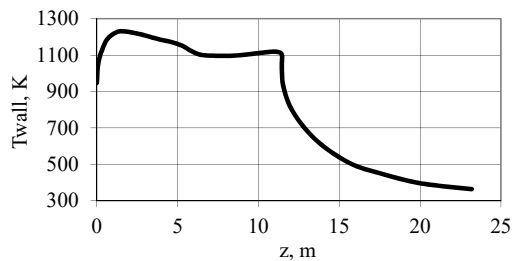


Fig. 10. Temperature on the inner surface of the refractory wall of the cooler drum with a thickness of 50 mm depending on its length (the length of the hot zone of the drum is 11.5 m)

From Fig. 11, 12, as well as for the BC of the I kind, it is seen that the maximum values of the mole fractions of the combustible components of the syngas are observed mainly in the cooling zone and in the outlet part of the drum, while non-combustible ones, on the contrary, are minimal. According to the calculations, the performance of the syngas cooler drum at the O₂/C ratio=48.5 % under normal conditions is 1,485 m³/hour.

As can be seen from Fig. 13, the results of calculations of the quantitative composition of the syngas at the outlet of the cooler drum by various programs for BC of the III kind, as well as for BC of the I kind, match.

The difference between the mole fractions of CO and H₂ at the O₂/C ratio=48.5% is in the range of (2.8–3.4) %.

The quantitative composition of the syngas at the outlet of the cooler drum was obtained for the BC of the III kind close to the quantitative composition of the syngas obtained

for the BC of the I kind. The difference between the values is: for CO – 4.1 % and for H₂ – 1.2 %.

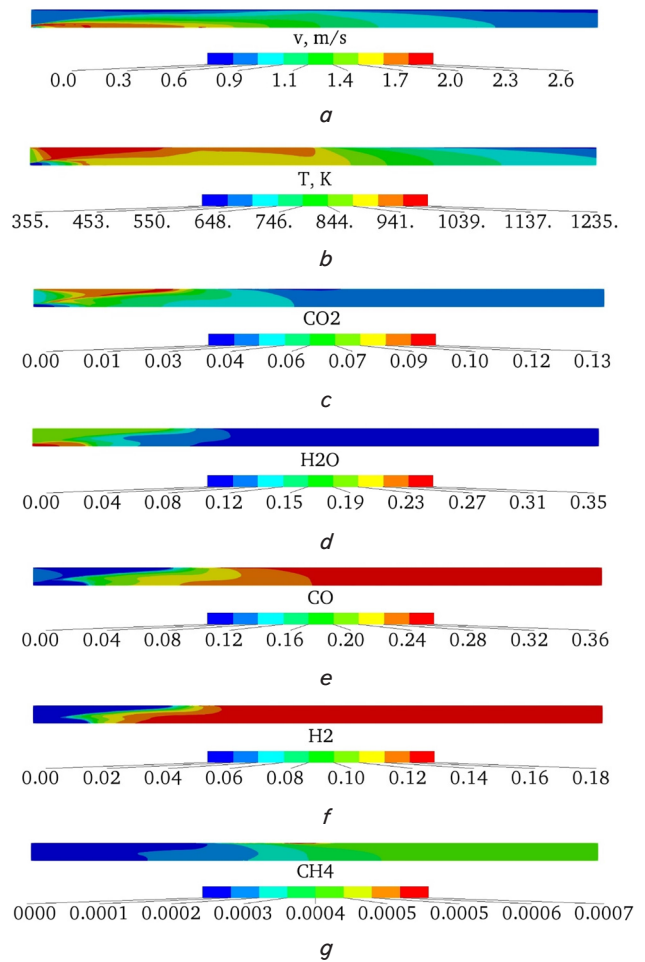


Fig. 11. Physical fields during gasification of the dust fraction of carbon-containing filler under boundary conditions of the III kind, the length of the isothermal zone of the drum of 11.5 m and the O₂/C ratio=48.5 %: a – velocity; b – temperature; c – CO₂ mole fraction; d – H₂O mole fraction; e – CO mole fraction; f – H₂ mole fraction; g – CH₄ mole fraction

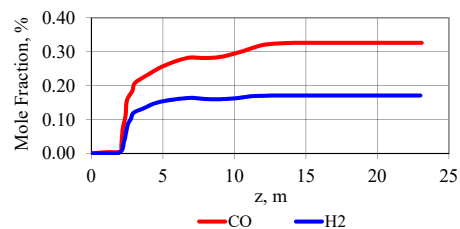


Fig. 12. Distribution of the mole fractions of the main combustible components of the syngas CO and H₂ along the axis of the cooler drum, boundary conditions of the III kind, the length of the hot zone of the drum is 11.5 m and the O₂/C ratio=48.5 %

An analysis of the results shows the following:

– if a cooler drum is used to generate syngas, it is necessary to rationally combine two different functions – the combustion chamber and the refrigerator. On the one hand, there must be a high-temperature zone in the cooler drum for generating syngas with a high output of combustible compo-

nents, and on the other hand, a cooling zone for obtaining material with a given temperature at the output;

– the obtained calculation data confirm the possibility of using industrial equipment – a cooler drum of a rotary kiln for calcining carbon-containing filler to generate syngas by burning production waste – the dust fraction of carbon material and the heat of the material coming from the rotary kiln to the cooler drum. For the ratio of $O_2/C=(42.7 \dots 51.6) \%$; the predicted quantitative composition of the syngas combustible gases in mole fractions is $CO=(32.8 \dots 36.9) \%$, $H_2=(17.1 \dots 18.4) \%$ and $CH_4=(0.03 \dots 0.16) \%$;

– the reliability of the results is confirmed by verification of the calculation data performed using the Fluent software product, with the calculation data in the equilibrium chemistry approximation using the NASA CEA program. The difference between the mole fractions of CO and H_2 , the value of which is obtained with various software products, is in the range of $(2.8 \dots 5.8) \%$. According to the calculations, the performance of the syngas cooler drum according to normal conditions is about $1,500 \text{ m}^3/\text{h}$ with a calorific value of $6.1 \text{ MJ}/\text{m}^3$;

– according to the known values of pressure, temperature and quantitative mass composition of the starting products (reagents), for the operational forecast of the quantitative composition of the syngas that is formed in the rotary kiln cooler drum and other industrial kiln equipment, NASA CEA software can be used.

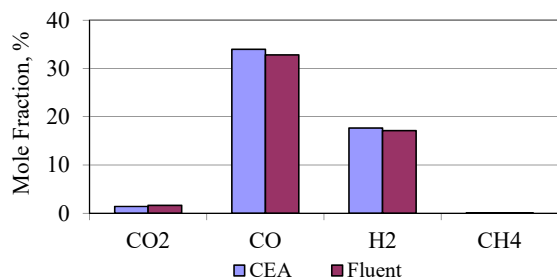


Fig. 13. Comparison of the quantitative composition of the syngas at the outlet of the rotary kiln cooler drum under boundary conditions of the III kind and the length of the hot zone of 11.5 m at the ratio $O_2/C=48.5 \%$, obtained using the Fluent and CEA software products

7. Discussion of the results of the study of the process of syngas generation in the rotary kiln cooler drum

The proposed method (1)–(6) (Tables 1, 2, Fig. 1, 2) allowed evaluating the feasibility of using the cooler drum to generate syngas as an alternative fuel for heat treatment of carbon-containing material in a rotary kiln (Fig. 3–7, 9, 11, 13). The reliability of the obtained data was confirmed by verification of the results of calculations using the software

product ANSYS Fluent [18] with the data of calculations by the NASA CEA program [20].

The available scientific literature [1–14, 17, 22, 23] does not reveal the results of both theoretical and experimental studies of the process of gasification of the dust fraction of carbon-containing material in the rotary kiln cooler drum. Thanks to the research using the developed numerical model, the possibility of conducting the process of gasification of carbon-containing material not in specialized equipment, but directly in the technological one, in particular in the rotary kiln cooler drum, is substantiated.

It is shown that the NASA CEA program [20], designed for operational calculations of equilibrium chemistry, can be used for engineering calculations of the material composition of syngas of industrial furnace equipment.

The considered method is based on the solution of an axisymmetric problem, which limits the practical application of this method, but at the same time significantly minimizes the requirements for computing and time resources.

The disadvantage of this study is the lack of consideration of the rotation of the cooler drum of the kiln, which affects the process of heat exchange between the bulk medium and the gas.

Further research is planned to be performed in the areas of solving the three-dimensional problem of the gasification process and experimental verification of the obtained theoretical results.

8. Conclusions

1. A mathematical model of the process of gasification of carbon particles is formulated in a continually discrete setting, including thirteen global reactions, of which four are heterogeneous and nine are homogeneous.

2. A numerical model for the gasification of the dust fraction of carbon-containing filler in the rotary kiln cooler drum in the axisymmetric formulation was developed. The convergence of the numerical solution of the gasification problem by the grid step is investigated. It is found that the computational grid, which includes 73,620 cells and 75,202 nodes, leads to an error in determining the main parameters of the model no more than 1–2 %.

3. Using the developed numerical model, the possibility of implementing the process of gasification of carbon-containing filler in the rotary kiln cooler drum was evaluated. It was found that at the O_2/C ratio $= (42.7 \dots 51.6) \%$, the predicted quantitative composition of syngas combustible gases in mole fractions is $CO=(32.8 \dots 36.9) \%$, $H_2=(17.1 \dots 18.4) \%$ and $CH_4=(0.03 \dots 0.16) \%$.

Verification of the developed numerical model is performed. It was found that the difference between the molar fractions of CO and H_2 , the values of which were obtained with different software products (Fluent, NASA CEA), is in the range of $(2.8 \dots 5.8) \%$.

References

1. Liu, X. J., Zhang, W. R., Park, T. J. (2001). Modelling coal gasification in an entrained flow gasifier. *Combustion Theory and Modelling*, 5 (4), 595–608. doi: <https://doi.org/10.1088/1364-7830/5/4/305>
2. Choi, Y. C., Li, X. Y., Park, T. J., Kim, J. H., Lee, J. G. (2001). Numerical study on the coal gasification characteristics in an entrained flow coal gasifier. *Fuel*, 80 (15), 2193–2201. doi: [https://doi.org/10.1016/s0016-2361\(01\)00101-6](https://doi.org/10.1016/s0016-2361(01)00101-6)
3. Shi, S.-P., Zitney, S. E., Shahnam, M., Syamlal, M., Rogers, W. A. (2006). Modelling coal gasification with CFD and discrete phase method. *Journal of the Energy Institute*, 79 (4), 217–221. doi: <https://doi.org/10.1179/174602206x148865>

4. Watanabe, H., Otaka, M. (2006). Numerical simulation of coal gasification in entrained flow coal gasifier. *Fuel*, 85 (12-13), 1935–1943. doi: <https://doi.org/10.1016/j.fuel.2006.02.002>
5. Wu, Y., Zhang, J., Smith, P.J., Zhang, H., Reid, C., Lv, J., Yue, G. (2010). Three-Dimensional Simulation for an Entrained Flow Coal Slurry Gasifier. *Energy & Fuels*, 24 (2), 1156–1163. doi: <https://doi.org/10.1021/ef901085b>
6. Liu, H., Cattolica, R. J., Seiser, R. (2017). Operating parameter effects on the solids circulation rate in the CFD simulation of a dual fluidized-bed gasification system. *Chemical Engineering Science*, 169, 235–245. doi: <https://doi.org/10.1016/j.ces.2016.11.040>
7. Zhang, Y., Lei, F., Xiao, Y. (2015). Computational fluid dynamics simulation and parametric study of coal gasification in a circulating fluidized bed reactor. *Asia-Pacific Journal of Chemical Engineering*, 10 (2), 307–317. doi: <https://doi.org/10.1002/apj.1878>
8. Zhong, W., Yu, A., Zhou, G., Xie, J., Zhang, H. (2016). CFD simulation of dense particulate reaction system: Approaches, recent advances and applications. *Chemical Engineering Science*, 140, 16–43. doi: <https://doi.org/10.1016/j.ces.2015.09.035>
9. Wu, Y., Liu, D., Ma, J., Chen, X. (2017). Three-Dimensional Eulerian–Eulerian Simulation of Coal Combustion under Air Atmosphere in a Circulating Fluidized Bed Combustor. *Energy & Fuels*, 31 (8), 7952–7966. doi: <https://doi.org/10.1021/acs.energyfuels.7b01084>
10. Sharma, V., Agarwal, V. K. (2019). Numerical simulation of coal gasification in a circulating fluidized bed gasifier. *Brazilian Journal of Chemical Engineering*, 36 (3), 1289–1301. doi: <https://doi.org/10.1590/0104-6632.20190363s20180423>
11. Peng, L., Wu, Y., Wang, C., Gao, J., Lan, X. (2016). 2.5D CFD simulations of gas–solids flow in cylindrical CFB risers. *Powder Technology*, 291, 229–243. doi: <https://doi.org/10.1016/j.powtec.2015.12.018>
12. Chui, E. H., Majeski, A. J., Lu, D. Y., Hughes, R., Gao, H., McCalden, D. J., Anthony, E. J. (2009). Simulation of entrained flow coal gasification. *Energy Procedia*, 1 (1), 503–509. doi: <https://doi.org/10.1016/j.egypro.2009.01.067>
13. Panov, E. N., Karvatskii, A. Y., Shilovich, T. B., Lazarev, T. B., Moroz, A. S. (2014). Mathematical Model of Solid-Fuel Gasification in a Fluidized Bed. *Chemical and Petroleum Engineering*, 50 (5-6), 312–322. doi: <https://doi.org/10.1007/s10556-014-9900-3>
14. Anetor, L., Osakue, E., Odetunde, C. (2012). Reduced Mechanism Approach of Modeling Premixed Propane-Air Mixture Using ANSYS Fluent. *Engineering Journal*, 16 (1), 67–86. doi: <https://doi.org/10.4186/ej.2012.16.1.67>
15. Gri mech 3.0 chemkin. Available at: <http://combustion.berkeley.edu/gri-mech/version30/files30/grimech30.dat>
16. Cantera is an open-source suite of tools for problems involving chemical kinetics, thermodynamics, and transport processes. Available at: <https://cantera.org/>
17. Slavinskaya, N., Braun-Unkhoff, M., Frank, P. (2008). Reduced Reaction Mechanisms for Methane and Syngas Combustion in Gas Turbines. *Journal of Engineering for Gas Turbines and Power*, 130 (2). doi: <https://doi.org/10.1115/1.2719258>
18. ANSYS. Available at: <https://www.ansys.com/>
19. MFIX. Available at: <https://mfix.netl.doe.gov/>
20. McBride, B. J., Gordon, S. (1996). Computer Program for Calculation of Complex Chemical Equilibrium Compositions and Applications II. Users Manual and Program Description. NASA RP 1311. National Aeronautics and Space Administration.
21. Chalyh, E. F. (1972). *Tehnologiya i oborudovanie elektrodnyh i elektrougol'nyh predpriyatij*. Moscow: Metallurgiya, 432.
22. Westbrook, C. K., Dryer, F. L. (1981). Simplified Reaction Mechanisms for the Oxidation of Hydrocarbon Fuels in Flames. *Combustion Science and Technology*, 27 (1-2), 31–43. doi: <https://doi.org/10.1080/00102208108946970>
23. Tahir, F., Ali, H., Baloch, A. A. B., Jamil, Y. (2019). Performance Analysis of Air and Oxy-Fuel Laminar Combustion in a Porous Plate Reactor. *Energies*, 12 (9), 1706. doi: <https://doi.org/10.3390/en12091706>
24. ParaView. An open-source, multi-platform data analysis and visualization application. Available at: <http://www.paraview.org/>